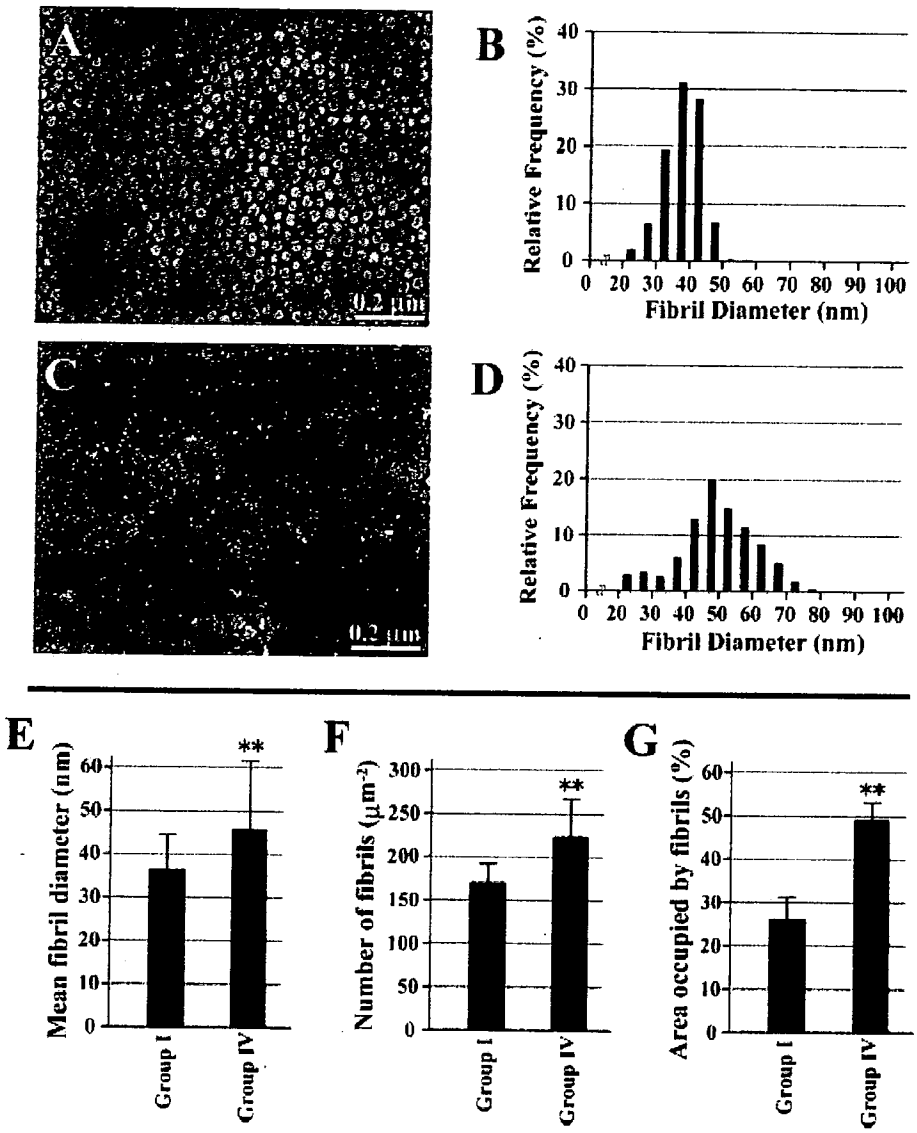

Figure 3. In the upper panel, photomicrographs of the repair tissue and the histograms for the distribution of fibril diameter in Group I (A and B) and Group IV (C and D) are shown. Fibril diameter (E), number of fibrils in a 1 μm square (F), and percentage of the area occupied by collagen fibril cross sections (G) of both groups are shown in the lower panel. The evaluation was performed on three animals in each group. Values are expressed by means + SD. $^{**}p < 0.01$ against Group I.

significantly reduced in Group IV ($p < 0.01$; Fischer's PLSD test) (Fig. 5D), and the expression of fibromodulin was remarkably suppressed in both GDF-5–treated groups ($p < 0.01$ for both groups; Fischer's PLSD test) (Fig. 5E). However, GDF-5 strongly stimulated the expression of lumican ($p < 0.01$ for both groups; Fischer's PLSD test) (Fig. 5F). When the expression of SLRPs was considered relative to type I collagen expression, the GDF-5 treatment strongly suppressed the expression of decorin and fibromodulin ($p < 0.01$ for both groups for both genes; Fischer's PLSD test) (Fig. 5G and H, respectively), while lumican expression was almost unaffected (Fig. 5I).

DISCUSSION

In this study, the results of biomechanical testing have shown that the process of ligament healing

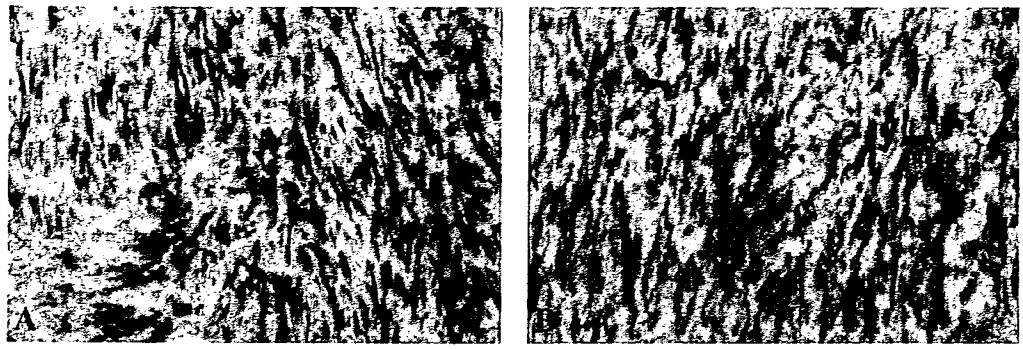

Figure 4. Results of in situ hybridization for pro α1(I) collagen mRNA in the repair tissues in Group I (A) and Group IV (B). Three animals in each group were evaluated at each time point, and representative photomicrographs of 1-week specimens are shown. Nuclei were stained with methyl green. Original magnification ×100. [Color scheme can be viewed in the online issue, which is available at http://www.interscience.wiley.com]

was in fact facilitated by GDF-5. Although a slight improvement was observed with the fibrin sealant alone, the data showed that the mechanical properties of the femur–MCL–tibia complex were significantly improved by 30 μg of GDF-5; the ultimate tensile strength of the complex was over 40% greater than that of the vehicle controls, and the stiffness was improved by 60%. The changes were both above the level of statistical significance. In all specimens, the failure occurred through the ligament midsubstance, and the result was attributed to the improved mechanical property of the healing tissue by GDF-5. A possible explanation for the positive effect was given by the results of in situ hybridization and quantitative PCR. These experiments revealed that the expression of type I procollagen genes was promoted in the healing tissue treated with GDF-5. Because type I collagen is the primary component of the repair tissue,[14] it is likely that the elevated type I collagen production led to an increase of repair tissue volume, giving higher mechanical strength to the tissue. Interestingly, the growth factor did not change the expression level of type III collagen, and thus, the expression of type III collagen relative to type I declined significantly. It is known that the ligament repair tissue contains an increased amount of type III collagen compared with a normal ligament,[14,15] which might be responsible for the poor mechanical property of the tissue.[16,17] Therefore, in this study, the relative decrease in type III collagen content might be related to the improvement of biomechanical results by altering the type I and type III collagen ratio toward normal.

The result of electron microscopic observation has shown another possible mechanism for the improved healing by GDF-5. In comparison to the controls, the repair tissue in the GDF-5–treated animals tended to contain thicker collagen fibrils at a higher density. Considering that the collagen fibril diameter is known to be a major determinant of the mechanical property of the ligaments,[18,19] the positive result might be the consequence of the increased size and density of collagen fibrils in the repair tissue.

The results of ultrastructural observation led us to examine the expression of small leucine-rich proteoglycans because they have been reported to affect collagen fibril formation in vivo.[20–22] In the present study, the expression of these genes was evaluated 1 week after surgery, the time point when the influence of GDF-5 on the healing process was most obvious by histology and in situ hybridization. The quantitative PCR analysis revealed that the effect of the growth factor varies on the genes; the expression of fibromodulin was strongly suppressed, lumican was enhanced, and decorin was not altered significantly. Because fibromodulin and lumican share similar effects on collagen fibrillogenesis,[21] the result did not seem to support the increase in the fibril size by GDF-5. Then, considering that these molecules modulate fibrillogenesis through the direct binding to collagen fibrils,[22] we obtained the expression ratios between the proteoglycans and type I procollagen. The results showed that the expression of decorin and fibromodulin were relatively suppressed, while the expression of lumican was nearly unaffected. Considering that these proteoglycans could inhibit collagen fibril assembly in the early phase of fibrillogenesis,[21,23] we currently presume that the relative suppression of decorin and fibromodulin could be related to the

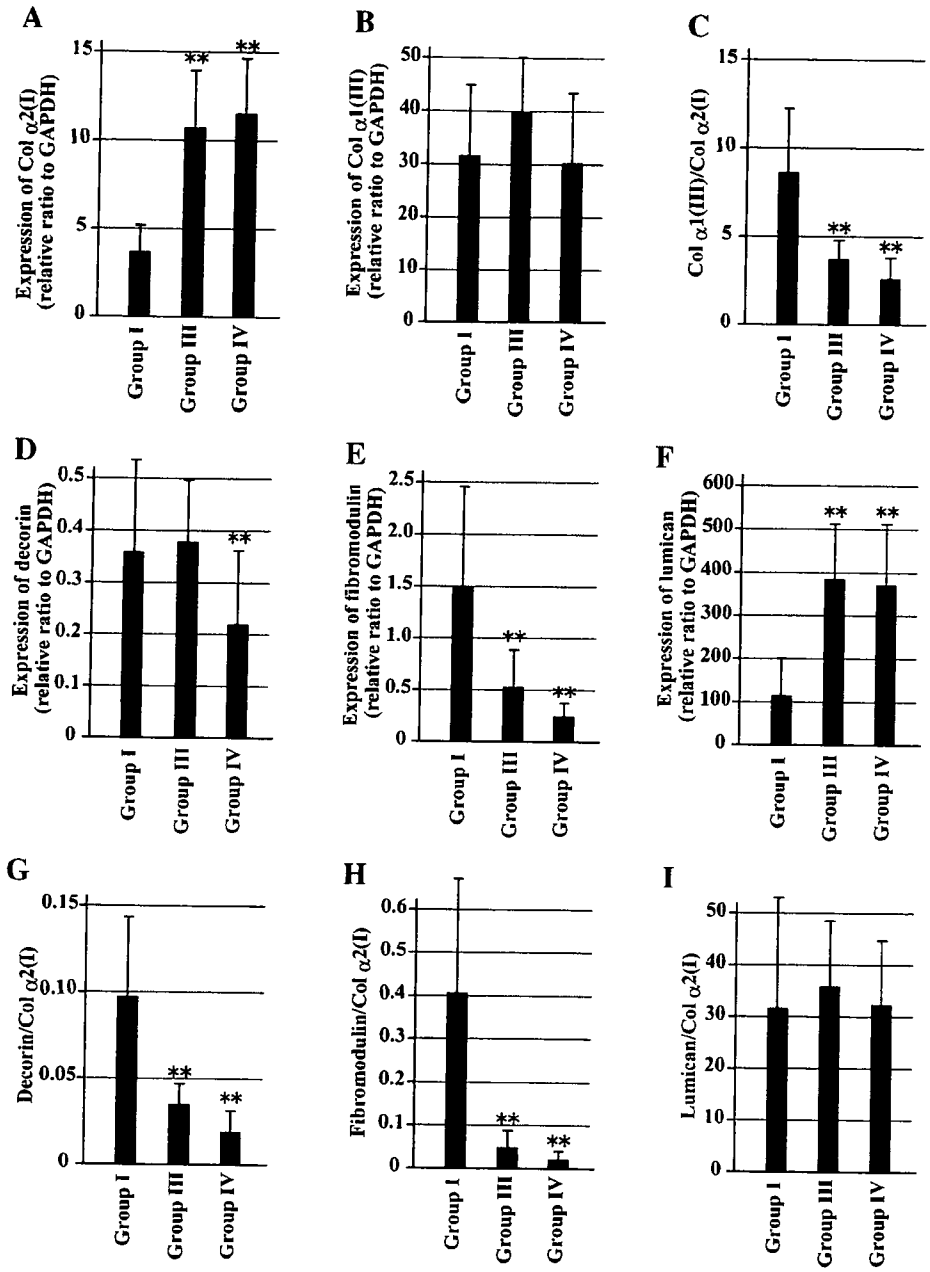

Figure 5. Result of quantitative PCR. Top panel shows the expression of pro α2(I) collagen (A), pro α1(III) collagen (B), and their expression ratios (C). Middle panel shows the expression of decorin (D), fibromodulin (E), and lumican (F) relative to GAPDH. Their expression ratios against pro α2(I) collagen are shown at the bottom panel (G–I, respectively). Each bar represents the average of five specimens. Values are expressed by means + SD. $*p < 0.05$, and $**p < 0.01$ against Group I.

appearance of thicker collagen fibrils by GDF-5. Similar data have been shown by a recent study that BMP-12, another member of the GDF family, suppressed decorin expression and elevated collagen expression in cultured human tendon fibroblasts.[24]

Collectively, exogenously added GDF-5 enhanced healing of an injured ligament histologically and biomechanically. No adverse effect was observed, and the use of GDF-5 was considered to be a promising approach to facilitate ligament healing.

ACKNOWLEDGMENTS

This work was supported in part by Grants-in-Aid from the Japan Society for the Promotion of Science (15390467) and the Ministry of Education, Culture, Sports, Science, and Technology (16659416). No benefits in any form have been received or will be received from a commercial party related directly or indirectly to the subject of this article.

REFERENCES

1. Hildebrand KA, Woo SL-Y, Smith DW. 1998. The effects of platelet-derived growth factor-BB on healing of the rabbit medial collateral ligament. An in vivo study. Am J Sports Med 26:549–554.
2. Letson AK, Dahners LE. 1994. The effect of combinations of growth factors on ligament healing. Clin Orthop 308:207–212.
3. Fukui N, Katsuragawa Y, Sakai H, et al. 1998. Effect of local application of basic fibroblasts growth factor on ligament healing in rabbits. Rev Rheum Engl Ed 65:406–414.
4. Spindler KP, Dawson JM, Stahlman GC, et al. 2002. Collagen expression and biomechanical response to human recombinant transforming growth factor beta (rhTGF-β2) in the healing rabbit MCL. J Orthop Res 20:318–324.
5. Chang SC, Hoang B, Thomas JT, et al. 1994. Cartilage-derived morphogenetic proteins. J Biol Chem 269:28227–28234.
6. Wolfman NM, Hattersley G, Cox K, et al. 1997. Ectopic induction of tendon and ligament in rats by growth and differentiation factor-5, 6, and 7, members of the TGF-β gene family. J Clin Invest 100:321–330.
7. Clark RT, Johnson TL, Schalet BJ, et al. 2001. GDF-5 deficiency in mice leads to disruption of tail tendon form and function. Connect Tissue Res 42: 175–186.
8. Mikic B, Schalet BJ, Clark RT, et al. 2001. GDF-5 deficiency in mice alters the ultrastructure, mechanical properties and composition of the Achilles tendon. J Orthop Res 19:365–371.
9. Aspenberg P, Forslund C. 1999. Enhanced tendon healing with GDF-5 and 6. Acta Orthop Scand 70: 51–54.
10. Forslund C, Rueger D, Aspenberg P. 2003. A comparative dose–response study of cartilage-derived morphogenetic protein (CDMP)-1, -2 and -3 for tendon healing in rats. J Orthop Res 21:617–621.
11. Rickert M, Jung M, Adiyaman M, et al. 2001. A growth and differentiation factor-5 (GDF-5)-coated suture stimulates tendon healing in an Achilles tendon model in rats. Growth Factors 19:115–126.
12. Chimich D, Frank C, Shrive N, et al. 1991. The effect of initial end contact on medial collateral ligament healing: a morphological and biomechanical study in a rabbit model. J Orthop Res 9: 37–47.
13. Frank CB, Bray D, Rademaker A, et al. 1989. Electron microscopic quantification of collagen fibril diameters in the rabbit medial collateral ligament: a baseline for comparison. Connect Tissue Res 19:11–25.
14. Frank CB, Amiel D, Woo SL-Y, et al. 1985. Normal ligament properties and ligament healing. Clin Orthop 196:15–25.
15. Amiel D, Frank CB, Harwood FL, et al. 1987. Collagen alteration in medial collateral ligament healing in a rabbit model. Connect Tissue Res 16: 357–366.
16. Eriksen HA, Pajala A, Leppilahti J, et al. 2002. Increased content of type III collagen at the rupture site of human Achilles tendon. J Orthop Res 20: 1352–1357.
17. Liu X, Wu H, Byrne M, et al. 1997. Type III collagen is crucial for collagen I fibrillogenesis and for normal cardiovascular development. Proc Natl Acad Sci USA 94:1852–1856.
18. Frank C, McDonald D, Bray D, et al. 1992. Collagen fibril diameters in the healing adult rabbit medial collateral ligament. Connect Tissue Res 27:251–263.
19. Frank C, McDonald D, Shrive N. 1997. Collagen fibril diameters in the rabbit medial collateral ligament scar: a longer term assessment. Connect Tissue Res 36:261–269.
20. Danielson KG, Baribault H, Holmes DF, et al. 1997. Targeted disruption of decorin leads to abnormal collagen fibril morphology and skin fragility. J Cell Biol 136:729–743.
21. Ezura Y, Chakravarti S, Oldberg Å, et al. 2000. Differential expression of lumican and fibromodulin regulate collagen fibrillogenesis in developing mouse tendons. J Cell Biol 151:779–787.
22. Iozzo RV. 1999. The biology of the small leucine-rich proteoglycans. Functional network of interactive proteins. J Biol Chem 274:18843–18846.
23. Naeme PJ, Kay CJ, McQuillan DJ, et al. 2000. Independent modulation of collagen fibrillogenesis by decorin and lumican. Cell Mol Life Sci 57:859–863.
24. Fu SC, Wong YP, Chan BP, et al. 2003. The roles of bone morphogenetic protein (BMP) 12 in stimulating the proliferation and matrix production of human patellar tendon fibroblasts. Life Sci 72: 2965–2974.

J Orthop Sci (2006) 11:159–166
DOI 10.1007/s00776-005-0988-3

JOURNAL OF
ORTHOPAEDIC SCIENCE

Original article

Endoscopic anterior cruciate ligament reconstruction using a computer-assisted fluoroscopic navigation system

HISATADA HIRAOKA[1,2], SOU KURIBAYASHI[1], AKIRA FUKUDA[1], NAOSHI FUKUI[1], and KOZO NAKAMURA[1]

[1]Department of Orthopaedic Surgery, The University of Tokyo, Tokyo, Japan
[2]Department of Orthopaedic Surgery, Saitama Medical Center, Saitama Medical School, 1981 Kamoda-tsujido, Kawagoe, Saitama 350-0844, Japan

Abstract

Background. During anterior cruciate ligament (ACL) reconstruction, placement of the reconstructed ligament affects the clinical results. To accomplish accurate and reproducible placement of the tibial bone tunnel, we employed a fluoroscopic navigation system for endoscopic ACL reconstruction. In this study, preciseness of the tibial tunnel placement was evaluated, and the advantages and disadvantages of this navigation system for endoscopic ACL reconstruction are discussed.

Methods. Altogether, 16 knees of 16 patients who had undergone ACL reconstruction using this system (navi group) were evaluated regarding the positioning of the tibial tunnel against Blumensaat's line using X-p and the route of the graft by magnetic resonance imaging (MRI). Another 16 knees of 16 patients who underwent endoscopic ACL reconstruction without the navigation system were the controls (control group).

Results. At the 1-year follow-up, maximally extended lateral knee X-p revealed that the anterior edge of the tibial tunnel and Blumensaat's line were almost aligned and that roof impingement was avoided; the T2-weighted MR images showed that the graft was placed close to and parallel to the intercondylar roof in all the knees of the navi group. The ratio of the distance between Blumensaat's line and the anterior edge of the tibial tunnel at the level of the tibial plateau to the anteroposterior width in fully extended true lateral radiographs was 2.7% ± 3.4% in the navi group and 8.4% ± 7.4% in the control group.

Conclusions. The computer-assisted fluoroscopic navigation system improves accuracy and decreases dispersion of the tibial tunnel placement against Blumensaat's line in single-bundle ACL reconstruction. This innovative device renders the reconstruction procedure more reliable, eliminating the problem of skeletal variation among patients. However, the function of this navigation system for femoral tunnel placement is insufficient at present. Further refinement of the system is necessary, and the method of application requires improvement.

Offprint requests to: H. Hiraoka
Received: May 2, 2005 / Accepted: November 8, 2005

Introduction

The current standard surgical procedure for treating the injured anterior cruciate ligament (ACL) is endoscopic reconstruction with autologus tissues. Although the surgery has become a common procedure for orthopedic surgeons, it is not easy to consistently obtain the best possible results. A recent report has shown that nearly 30% of ACL-reconstructed knees had more than 3 mm of side-to-side difference even though the surgery was performed by an experienced surgeon.[1] There are various reasons for failure: choice of the graft, graft tension at the time of fixation, method of fixation, and rehabilitation protocols. Among them, proper graft placement is a critical factor for successful reconstruction.[2–4] If a graft is misplaced, it often fails because of roof impingement[5,6] or poor isometry, or it may cause loss of knee motion long after surgery.

The navigation system is a computer-assisted surgery system that has recently been introduced in the operating room. Currently, the most common type of system is an image-guided navigation system based on fluoroscopy or CT images. During surgery, the system indicates the location of the surgical instrument on the images obtained before surgery, eliminating the need for intraoperative image acquisition.

In the field of orthopedic surgery, the method has been used for spinal surgery,[7–11] prosthetic surgery of the hip and knee joints,[12–17] and trauma surgery,[18–20] and successful results have been reported. Its application in ACL reconstruction surgery has also been proposed.[21–24] For ACL surgery, the system is expected to display virtual images of bone tunnels and the graft on radiographic or computed tomography (CT) images before the bone tunnels are drilled, allowing the surgeon to place the graft in the optimal position. However, its feasibility and usefulness in clinical practice has not yet been determined.

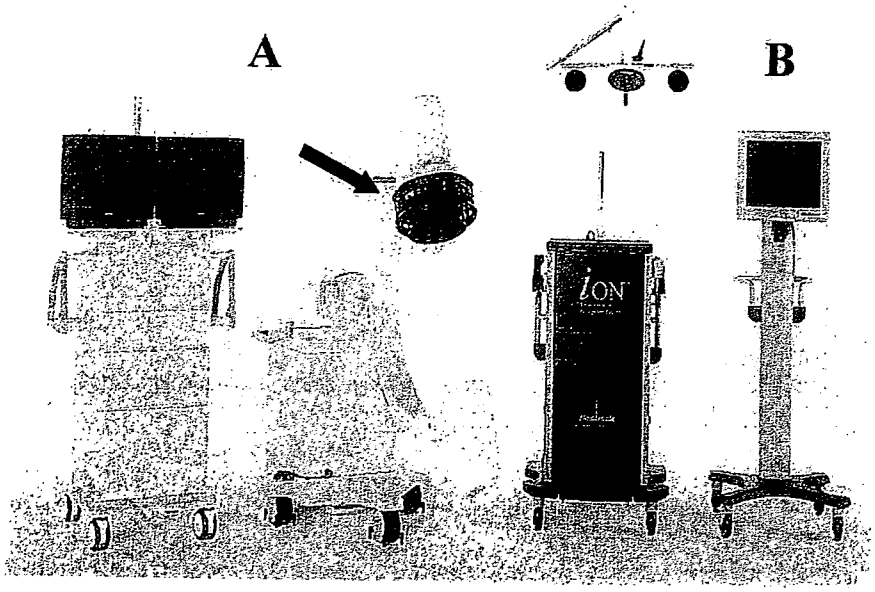

Fig. 1. Configuration of the navigation system used for the study. The system consists of a C-arm fluoroscopy (**A**) with a calibration target (*arrow*) and a core machine equipped with a digitizing camera and a screen for navigation (**B**)

Since October 2001, we have employed a navigation system based on fluoroscopic images for endoscopic ACL reconstruction. Because the system displays the predicted positions of the tibial bone tunnel and the route of the ligament graft in real time before the guide pin is inserted, the surgeon can easily place the graft in the expected, optimal position. We have introduced our endoscopic ACL reconstruction method using a fluoroscopy-based navigation system.[25] In this study the preciseness of the positioning of the tibial tunnel and the graft route were evaluated. The advantages and disadvantages of this navigation system in endoscopic ACL reconstruction are discussed here.

Materials and methods

The study was performed with the approval of the institutional review board, and all patients signed the consent form drafted for the study.

Between October 2001 and April 2003, 17 knees in 17 patients (10 male, 6 female; average age 26.9 ± 9.0 years at the time of surgery) underwent endoscopic ACL reconstruction using the fluoroscopic navigation system by three senior surgeons, and were involved in this study (navi group). Two patients had bilateral ACL injuries, and the other 15 had unilateral injuries. Another 16 patients (12 males, 4 females; average age 29.8 ± 8.9 years at the time of surgery) who underwent ACL reconstruction by the same senior surgeons without using navigation system just before the introduction of this navigation system served as the control group.

Navigation system

A computer-assisted fluoroscopic navigation system (StealthStation iON; Medtronic, Louisville, CO, USA) was used for the study (Fig. 1). This system is composed of a C-arm fluoroscope and a navigation system. The former has a C-arm with calibration target and a fluoroscopic monitor, and the latter has two devices consisting of a core machine with a digitizing camera, which localizes the C-arm calibration target and all of the trackable instruments, and the navigation display. The calibration target features light-emitting diode (LED) tracking to enable the precise localization of the C-arm. Up to four fluoroscopic images can be shown on the navigation display simultaneously, and virtual navigation images are overlaid on these images in a real-time manner. The mean probe tip error of this system was reported to be 0.97 ± 0.40 mm.[11]

Two LED frames (Fig. 2) were sterilized and used for navigation in the surgical field. One frame was attached to a commercially available tibial drill guide (Atlantech Medical Devices, Harrogate, N. Yorkshire, UK) with a universal tool adapter (Fig. 2A), and the other (Fig. 2B) was anchored securely to the midshaft of the tibia by two threaded pins (Fig. 3: reference frame). Fluoroscopic images were then obtained by the fluoroscope, with the calibration target and the reference frame captured simultaneously by the digitizing camera; the images were recorded. Finally, the tibial drill guide with the LED frame (Fig. 2A) was registered to the navigation system. After this step, the system traced LED markers of the ACL tibial guide and the reference

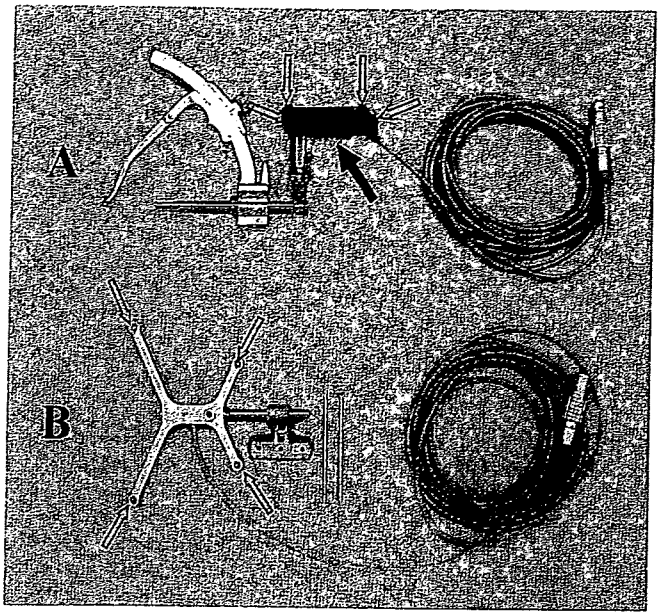

Fig. 2. Surgical instruments used for navigation. A tibial drill guide anchoring an active light-emitting diode (LED) frame (*black arrow*) with a universal tool adapter (**A**) and a reference frame (**B**) carrying active LED markers. The *open arrows* indicate the LED markers

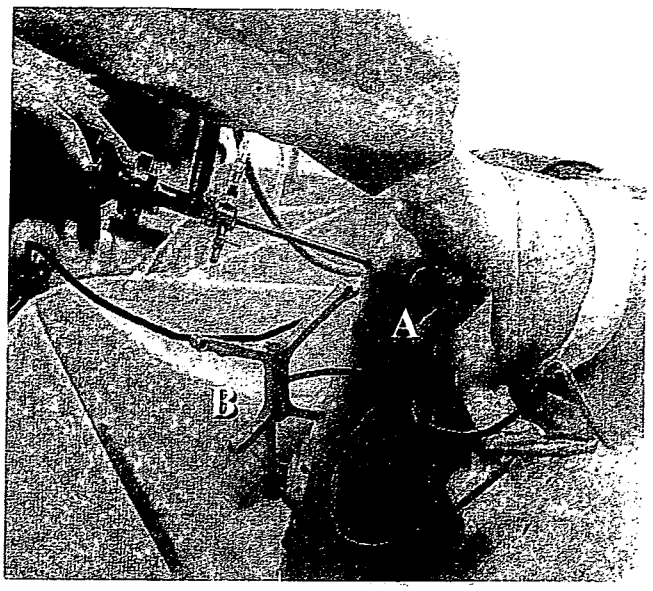

Fig. 3. Operation of the navigation system during surgery. A tibial drill guide (**A**) and reference frame on the tibia (**B**) are seen. Navigation can be performed by concurrently capturing the LED frame of the ACL drill guide (**A**) and the reference frame on the tibia (**B**) with the digitizing camera

frame on the tibia, indicating the virtual bone tunnel and graft route on the navigation images in a real-time manner, regardless of the actual position of the knee being operated on (Fig. 3).

Surgical procedure

Surgery started with endoscopic examination of the joint. Any treatment necessary for the menisci was performed prior to ACL reconstruction. A reference frame was then securely anchored to the midshaft of the tibia, and anteroposterior (AP) and lateral view images of the knee joint were obtained by C-arm fluoroscopy, capturing the calibration target and the reference frame simultaneously by the digitizing camera. To evaluate the risk of roof impingement properly, a lateral view image was obtained in the maximally extended knee position, and rotation of the joint was carefully confirmed by observing the overlap of medial and lateral femoral condyles. Registration of the tibial guide with the LED frame to the navigation system was then performed. Once this registration was completed, further use of fluoroscopy was not necessary for the navigation.

To prepare an ACL graft, semitendinosus and gracilis tendons were harvested and doubled in the middle. The diameter of the graft was measured and put into the navigation system; the system was then able to show the predicted positions of the tibial bone tunnel and the ACL graft route on the navigation images in the predicted graft diameter (Fig. 4). We placed the tibial tunnel where the extension of the anterior tunnel wall would come into line with the intercondylar roof (i.e., Blumensaat's line) (Fig. 4). For this, the position of the bone tunnel should be determined on the lateral knee images obtained at full joint extension in the exact orientation. The navigation system made this possible without changing the knee position or retaking the radiographic images. A guide pin was then driven through the navigated tibial guide. Finally, the tunnel was overreamed in the graft diameter along the guide pin. For the femoral socket, a guide pin was inserted using a size-specific offset aimer (Arthrotek, Warsaw, IN, USA) through the tibial tunnel, and the femoral socket was reamed in the graft diameter. We aimed the insertion point of the femoral guide pin at the 2 o'clock position on the left knee or at the 10 o'clock position on the right knee. After pretensioning, the ACL graft was placed and then fixed with a TransFix system (Arthrex, Naples, FL, USA) in the femoral socket and a spiked washer on the tibia at 20 degrees of knee flexion.

Postoperatively, continuous passive motion (CPM) was started immediately, and weight-bearing was begun as soon as tolerable, usually on the third day after surgery. The patients were encouraged to resume a full range of joint motion including Japanese-style sitting by 12 weeks. Jogging started at the fourth month, and return to full sports activity was permitted after 8 months at the earliest.

Fig. 4. Display of the navigation images on the navigation screen. Anteroposterior and true lateral images of full joint extension were obtained at the beginning of the surgery, and virtual tibial bone tunnel and the graft route images were then overlaid on the knee images at full joint extension in a real-time manner, irrespective of the actual knee position (e.g., Fig. 3)

Evaluations

The location of the tibial tunnel was evaluated on a lateral-view radiograph 12 months after surgery. The lateral-view radiograph was obtained in the maximally extended knee position, carefully confirming the rotation using a roentgen fluoroscope. On the lateral radiograph, the ratio of the absolute value of the distance between Blumensaat's line and the anterior edge of the tibial tunnel at the level of the tibial plateau to the AP width of the tibial plateau (Fig. 5, %B–A distance) was evaluated, and the absolute value of the angle between Blumensaat's line and the axis of the tibial tunnel (B–T angle) was measured (Fig. 5). Together with the radiographs, T2-weighted MR images were obtained on all knees at full extension, and the location and signal intensity of the grafts were evaluated.

To compare the accuracy of the tibial bone tunnel placement, the %B–A distance and the B–T angle of the patients in the control group was also measured on a lateral-view radiograph taken in the same manner as that of the navi group 12 months after surgery.

In addition, the side-to-side differences of the anterior instability measured by KT-1000/2000 at the 1-year follow-up were compared between the two groups.

Statistical analysis was performed using the Mann-Whitney U-test for the comparison of the two group and the F test for analysis of variance. Statistical significance was defined as $P < 0.05$.

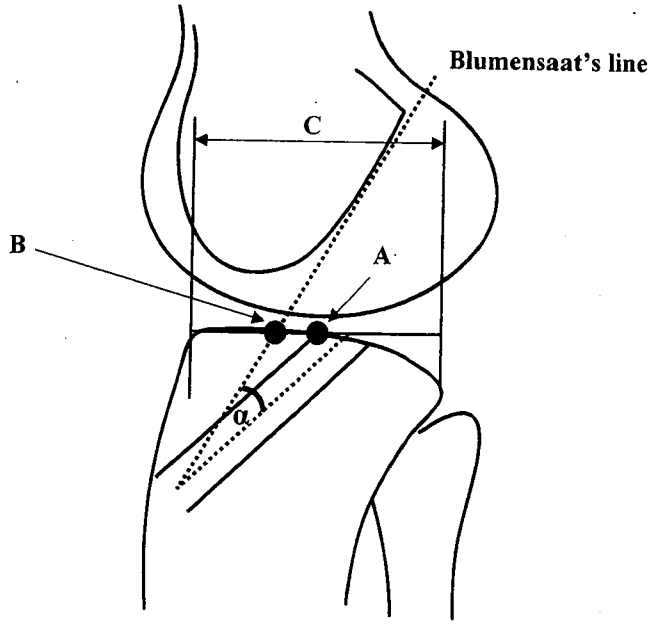

Fig. 5. Radiographic parameters used to evaluate the positioning of the tibial tunnel in this study. The %B–A distance is the ratio of the distance between Blumensaat's line and the anterior edge of the tibial tunnel at the level of the tibial plateau (*B–A*) to the anteroposterior width (*C*). The B–T angle is the angle between Blumensaat's line and the axis of the tibial tunnel (α)

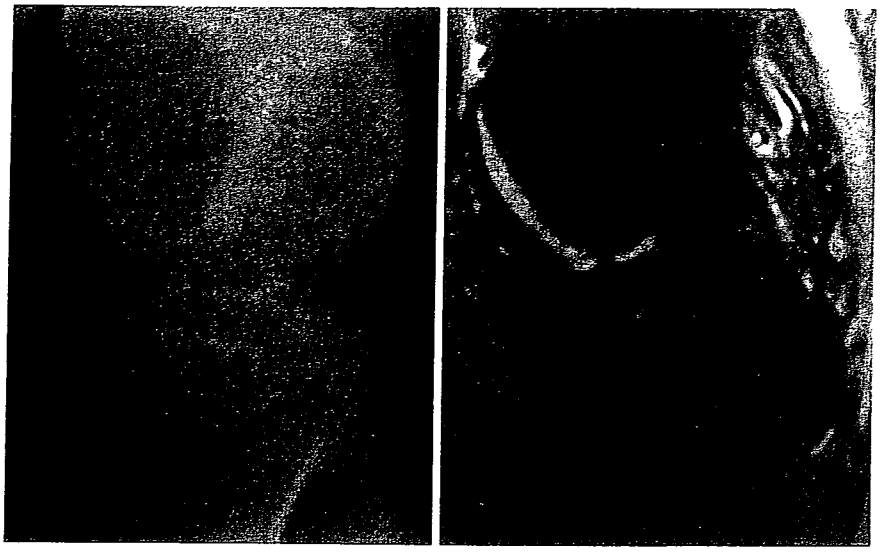

Fig. 6. Lateral radiograph (*left*) and T2-weighted magnetic resonance (MR) image (*right*) at full joint extension of a representative subject obtained 12 months after surgery. Roof impingement was avoided, and the MR image showed that the graft was located close to the intercondylar roof in a parallel orientation

Results

One patient who had a unilateral injury in the navi group was lost to the follow-up, and the remaining 16 knees of the 16 patients in the navi group and 16 knees of the 16 patients in the control group were enrolled in this study. In the navi group, two patients had ACL injuries in their bilateral knees but underwent unilateral reconstruction during the period; another two patients had concomitant meniscus injuries that were treated by partial meniscectomy. Still another patient had a grade III medial collateral ligament (MCL) injury that was repaired using a spiked washer. In the control group, four patients had meniscus injuries, two of which were treated by meniscectomy; and the others were repaired. One of them had a grade III MCL injury that was also repaired using the spiked washer technique. Surgery and the postoperative course were uneventful for all patients in both groups.

At the 1-year follow-up, physical examination revealed that full range of motion had been restored in all of the knees operated on in both groups. On the radiographs, there was no sign of abnormal widening of the tibial tunnels in either group. In the navi group, the lateral radiograph at full extension of the knee showed that the anterior wall of the tibial tunnel was located in line with or slightly behind the extension of the Blumensaat's line at the level of the tibial plateau in all the treated knees (Fig. 6), and successful avoidance of roof impingement was indicated. The %B–A distance and the B–T angle were 2.7% ± 3.4% and 4.8° ± 3.5° in the navi group, and 8.4% ± 7.4% and 6.0° ± 4.7° in the control group. The histogram of the %B–A distance is shown in Fig. 7. The mean and standard deviation of the %B–A distance in the navi group was significantly less than that in the control group ($P = 0.01$, 0.004, respectively) (Table 1).

Avoidance of roof impingement was also confirmed by MRI scans obtained at full extension of the knee in all subjects of the navi group at the 1-year follow-up. A sagittal view of T2-weighted MR images showed that the grafts were placed close to and parallel to the intercondylar roofs as normal anatomy (Fig. 6), and the grafts were depicted as low signal bands in all the patients, suggesting preservation of their structural integrity.

The side-to-side difference of anterior instability was measured in unilateral ACL-injured patients: 14 patients of the navi group and 16 of the control group. The average side-to-side difference was 1.3 ± 2.7 mm in the navi group and 1.3 ± 1.7 mm in the control group. There was no statistical difference between the two groups ($P = 0.95$).

Discussion

Despite their importance to ACL reconstruction, bone tunnels are often misplaced. Although there are several reasons, individual variation in joint geometry is probably a frequent cause of this problem. For example, the intercondylar roof angle varies from 22° to 64°,[26] and the extent of knee hyperextension can differ among individuals.

Because it is impossible to evaluate such variation by arthroscopy, the surgeon often needs to confirm the location of the guide pin by intraoperative radiography or fluoroscopy.[27] However, recognizing the exact pin position is difficult using regular radiography because the radiographs are often obtained in improper orienta-

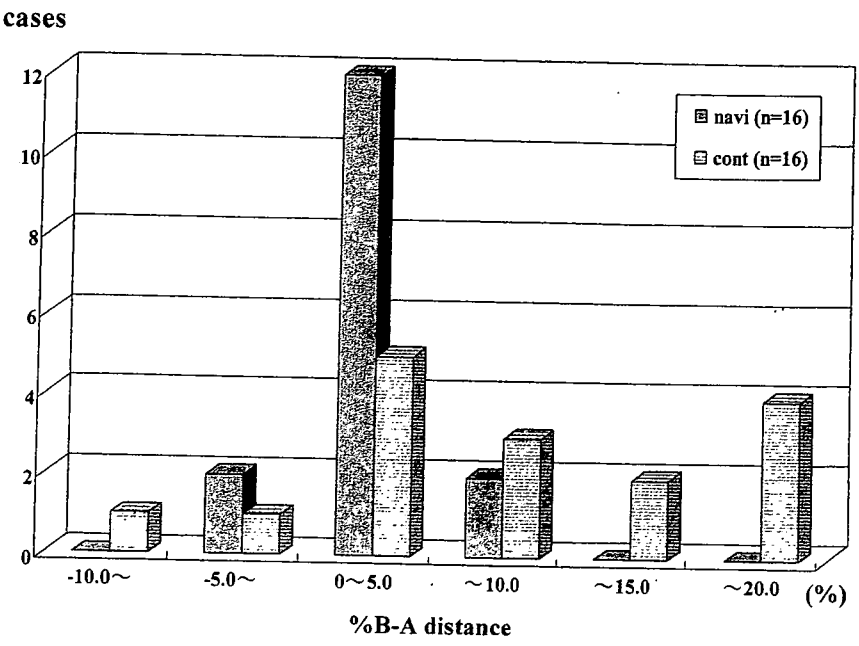

Fig. 7. Histogram of the %B–A distance. *navi*, navigation system; *cont*, controls

Table 1. %B–A distance and the B–T angle of the navigation (navi) and control groups

		Navi (n = 16)	Control (n = 16)	P value
%B–A distance (%)	Mean	2.7	8.4	*P = 0.01
	SD	3.4	7.4	*P = 0.004
B–T angle (degrees)	Mean	4.8	6.0	P = 0.65
	SD	3.5	4.7	P = 0.23

SD: standard deviation
*Significantly different ($P < 0.05$)

tion. Additionally, because either method shows the position of the guide pin that has already been placed, precise control of guide pin placement is difficult. To make a definitive decision about tibial tunnel placement by intraoperative fluoroscopy, it is necessary to predict the tunnel width of the graft diameter on the guide pin that is already in the tibia. Furthermore, reattempts of guide pin placement for slight transfer is difficult if the target point of the second guide pin is close to the first one. As a result, the surgeon compromises, and the guide pin shows a tendency to be placed posteriorly. With navigation, virtual tunnel placement can be superimposed on the strictly obtained AP and lateral views of the knee joint, and it is displayed in the actual diameter of the graft before guide pin insertion, as shown in Fig. 4. Therefore, strict guide pin placement can be easily accomplished during the first attempt.

Several articles have described the potential advantages of a navigation system for strict placement of the tunnel. Klos et al. developed a system that displays computer graphics of a virtual graft on a fluoroscopic image of the knee joint, and a clinical trial revealed that the technique statistically reduced the variability of ligament placement.[22] One limitation with the system was that it did not have a tracking system for the limb or the surgical instruments, and fluoroscopic images had to be acquired repeatedly during surgery. The virtual images had to be adjusted manually on the computer again when the limb position changed. Several other systems have been attempted on cadavers and plastic models, and accurate tunnel placement has been reported.[21,23,24] However, these methods require CT scanning for preoperative planning[21,23] or multiple intraoperative palpation of anatomical structures and landmarks around the joints.[24] Their value and feasibility have not yet been determined in clinical situations. Compared with these systems, the navigation system used in this study requires image acquisition only once, at the beginning of surgery; once the images have been recorded, operation of the system is simple. Because the virtual images are displayed on the knee images at full joint extension irrespective of the actual knee position, the surgeon does not have to extend the joint even to know the relation between the tunnel and Blumensaat's line during knee extension.

The results of this study show that the mean and standard deviation of the %B–A distance in the navi group were smaller than those in the control group (Table 1, Fig. 7). Particularly, the significantly decreased standard deviation of the %B–A distance in the

navi group was considered more meaningful. This means that not only stricter placement of the tibial tunnel in the navi group against Blumensaat's line but more reproducible placement of the bone tunnel can be accomplished than for that of the control group. In fact, lateral radiography in the fully extended knee position revealed that roof impingement was completely avoided in all knees of the navi group, and the tibial tunnels were placed immediately behind and almost parallel to Blumensaat's lines, whose tilt against the tibial plateau in the sagittal plane at full extension of the knee can vary from person to person. The sagittal view of T2-weighted MR images taken at full extension also showed that the grafts were placed close to and parallel with the intercondylar roofs as normal anatomy. We believe that the tibial tunnel being as anterior as possible and the graft lying close to Blumensaat's line at full knee extension is important for resuming the ligament's function, as it limits anterior instability and hyperextension of the joint.[28,29] Meanwhile, the %B–A distance of the two cases is more than 5%, as shown in Fig. 7. The LED frames attached to both the tibia and the tibial guide are highly sensitive to vibration and movement. This was thought to be due to erroneously touching the LED frames by the surgeon during surgery. Careful handling of the devices is required.

In this series of patients, the navigation system was not used for the femoral tunnel. There were two reasons for this. The first reason concerned the hardware and softwear. In the system we used, preparation for navigation including installing the LED frame into the bone, taking C-arm images used for navigation, and registering of the LED frames, which would have to be repeated for the tibia and femur, respectively. If navigation is planned for both tibia and femur, it would take twice as long to set up. Also, navigation for the femoral tunnel cannot be performed using the tunnel view because of the impossibility of obtaining that image on the operating room table, where we can determine the precise angle and placement of the femoral tunnel instead of the frontal image. The second reason is because precise femoral tunnel placement can be determined using a commercially available femoral offset guide that references definite bony landmarks of the over-the-top position and posterior edge of the lateral femoral condyle after complete removal of ACL remnants and the surrounding soft tissue. Therefore, we believe that using this particular navigation system for the femoral bone tunnel is not mandatory for single-bundle ACL reconstruction. Navigation based on strict lateral and tunnel views will be essential for accurate placement of the femoral tunnel in the next generation of devices.

Issues concerning clinical results, extra work, and surgeons for intraoperative navigation as well as the cost of the navigation system itself are also points of interest. The results of this study showed that there was no statistical difference in the side-to-side difference in anterior instability between the two groups if senior surgeons performed the surgery. Nowadays, however, ACL reconstruction has become a common procedure, so many orthopedic surgeons who sometimes perform arthroscopic surgery but are not familiar with ACL reconstruction sometimes perform this operation. This navigation technique should provide a significant aid for these surgeons.

Extra work for navigation is of course required. After preparation of the graft, two LED frames were anchored to the tibial guide and the midshaft of the tibia, respectively; fluoroscopic images were then obtained and the images recorded for navigation. Finally, the tibial drill guide with the LED frame was registered in the navigation system. These steps were performed during deflation of the tourniquet.

The average surgery time calculated in patients who underwent isolated ACL reconstruction with one senior surgeon without associated meniscus or MCL surgery was 152.7 ± 19.7 min (130–180 min) in the navi group ($n = 7$) and 119.7 ± 7.8 min (112–134 min) in the control group ($n = 6$). Therefore, the intraoperative time extension with fluoroscopic navigation for the tibial tunnel was about 30 min on average in this initial series. However, there was a learning curve regarding handling of the navigation system; when it was first introduced, it took more than an hour to set up, whereas at the end of this patient series setting up took less than 20 min. It has also been reported surgery time with the fluoroscopy-based navigation system for cup implantation in total hip arthroplasty was extended 13 min on average.[16] The involvement of an extra person, who assisted from outside of the operating field but did not have to be a surgeon, was necessary. Therefore, at the minimum, two orthopedic surgeons and an extra person were necessary for the procedure.

The introductory cost of the navigation system used in this study is approximately 30 million yen at listed price. However, the system is versatile; applications of this system in orthopedic surgery are spinal surgery,[10,11] total hip/knee arthroplasty,[16,17] and trauma surgery.[18–20] Once the fluoroscopic navigation system is introduced into the operating room, significant advantages can be enjoyed in an extensive field. Therefore, cost-effectiveness may be move realistic when operations other than ACL reconstruction utilize it.

Conclusions

The computer-assisted fluoroscopic navigation system improves accuracy and decreases dispersion of the tibial

tunnel placement against Blumensaat's line in single-bundle ACL reconstruction. This innovative device renders the reconstruction procedure more reliable, eliminating the problem of skeletal variation among patients. However, the function of this navigation system for femoral tunnel placement is insufficient at present. Further refinement of the system is necessary, and the method of application requires improvement.

Acknowledgements. The authors thank Professor Hiroya Sakai, MD, PhD for direction as well as Takumi Nakagawa, MD, PhD, Yoshinari Miyamoto, MD, and Takehiro Matsubara, MD for their assistance with this study.

No benefits in any form have been received or will be received from a commercial party related directly or indirectly to the subject of this article, nor have any funds been received in support of this study. The authors declare that this study complies with the laws of Japan.

References

1. Harner CD, Fu FH, Irrgang JJ, Vogrin TM. Anterior and posterior cruciate ligament reconstruction in the new millennium: a global perspective. Knee Surg Sports Traumatol Arthrosc 2001;9:330–6.
2. Friedman RL, Feagin JA Jr. Topographical anatomy of the intercondylar roof: a pilot study. Clin Orthop 1994;306:163–70.
3. Morgan CD, Kalman VR, Grawl DM. Definitive landmarks for reproducible tibial tunnel placement in anterior cruciate ligament reconstruction. Arthroscopy 1995;11:275–88.
4. Yaru NC, Daniel DM, Penner D. The effect of tibial attachment site on graft impingement in an anterior cruciate ligament reconstruction. Am J Sports Med 1992;20:217–20.
5. Howell SM, Clark JA. Tibial tunnel placement in anterior cruciate ligament reconstructions and graft impingement. Clin Orthop 1992;283:187–95.
6. Howell SM, Taylor MA. Failure of reconstruction of the anterior cruciate ligament due to impingement by the intercondylar roof. J Bone Joint Surg Am 1993;75:1044–55.
7. Arand M, Hartwig E, Kinzl L, Gebhard F. Spinal navigation in cervical fractures — a preliminary clinical study on Judet-osteosynthesis of the axis. Comput Aided Surg 2001;6:170–5.
8. Arand M, Hartwig E, Kinzl L, Gebhard F. Spinal navigation in tumor surgery of the thoracic spine: first clinical results. Clin Orthop 2002;399:211–8.
9. Nolte LP, Slomczykowski MA, Berlemann U, Strauss MJ, Hofstetter R, Schlenzka D, et al. A new approach to computer-aided spine surgery: fluoroscopy-based surgical navigation. Eur Spine J 2000;9(Suppl 1):S78–88.
10. Fu TS, Chen LH, Wong CB, Lai PL, Tsai TT, Niu CC, et al. Computer-assisted fluoroscopic navigation of pedicle screw insertion: an in vivo feasibility study. Acta Orthop Scand 2004;75:730–5.
11. Foley KT, Simon DA, Rampersaud YR. Virtual fluoroscopy: computer-assisted fluoroscopic navigation. Spine 2001;26:347–51.
12. DiGioia AM, Jaramaz B, Blackwell M, Simon DA, Morgan F, Moody JE, et al. Image guided navigation system to measure intraoperatively acetabular implant alignment. Clin Orthop 1998;355:8–22.
13. Digioia AM III, Jaramaz B, Plakseychuk AY, Moody JE Jr, Nikou C, LaBarca RS, et al. Comparison of a mechanical acetabular alignment guide with computer placement of the socket. J Arthroplasty 2002;17:359–64.
14. Leenders T, Vandevelde D, Mahieu G, Nuyts R. Reduction in variability of acetabular cup abduction using computer assisted surgery: a prospective and randomized study. Comput Aided Surg 2002;7:99–106.
15. Zheng G, Marx A, Langlotz U, Widmer K-H, Buttaro M, Nolte L-P. A hybrid CT-free navigation system for total hip arthroplasty. Comput Aided Surg 2002;7:129–45.
16. Hube R, Birke A, Hein W, Klima S. CT-based and fluoroscopy-based navigation for cup implantation in total hip arthroplasty (THA). Surg Technol Int 2003;11:275–80.
17. Victor J, Hoste D. Image-based computer-assisted total knee arthroplasty leads to lower variability in coronal alignment. Clin Orthop 2004;428:131–9.
18. Mosheiff R, Khoury A, Weil Y, Liebergall M. First generation computerized fluoroscopic navigation in percutaneous pelvic surgery. J Orthop Trauma 2004;18:106–11.
19. Grutzner PA, Suhm N. Computer aided long bone fracture treatment. Injury 2004;35:S-A57–64.
20. Mosheiff R, Weil Y, Khoury A, Liebergall M. The use of computerized navigation in the treatment of gunshot and shrapnel injury. Comput Aided Surg 2004;9:39–43.
21. Burkart A, Debski RE, McMahon PJ, Rudy T, Fu FH, Musahl V, et al. Precision of ACL tunnel placement using traditional and robotic techniques. Comput Aided Surg 2001;6:270–8.
22. Klos TVS, Habets RJE, Banks AZ, Banks SA, Devillee RJJ, Cook FF. Computer assistance in arthroscopic anterior cruciate ligament reconstruction. Clin Orthop 1998;354:65–9.
23. Picard F, DiGioia AM, Moody J, Martinek V, Fu FH, Rytel M, et al. Accuracy in tunnel placement for ACL reconstruction: comparison of traditional arthroscopic and computer-assisted navigation techniques. Comput Aided Surg 2001;6:279–89.
24. Sati M, Stäubli H-U, Bourquin Y, Kunz M, Nolte L-P. Real-time computerized in situ guidance system for ACL graft placement. Comput Aided Surg 2002;7:25–40.
25. Hiraoka H, Kuribayashi S, Nakagawa T. Anterior cruciate ligament reconstruction of the knee using fluoroscopic navigation system. Kansetugeka (Journal of Joint Surgery) 2005;24:84–9 (in Japanese).
26. Amis AA, Jakob RP. Anterior cruciate ligament graft positioning, tensioning and twisting. Knee Surg Sports Traumatol Arthrosc 1998;6(Suppl 1):S2–12.
27. Halbrecht J, Levy IM. Fluoroscopic assist in anterior cruciate ligament reconstruction. Arthroscopy 1993;9:533–5.
28. Cabaud HE. Biomechanics of the anterior cruciate ligament. Clin Orthop 1983;172:26–31.
29. Fuss FK. The restraining function of the cruciate ligaments on hyperextension and hyperflexion of the human knee joint. Anat Rec 1991;230:283–9.

Cell Tissue Res (2006) 323: 245–252
DOI 10.1007/s00441-005-0068-1

REGULAR ARTICLE

Sakae Sano · Akihiko Okawa · Arata Nakajima · Masamichi Tahara · Koji Fujita · Yuichi Wada · Masashi Yamazaki · Hideshige Moriya · Takahisa Sasho

Identification of *Pip4k2β* as a mechanical stimulus responsive gene and its expression during musculoskeletal tissue healing

Received: 16 December 2004 / Accepted: 26 July 2005 / Published online: 12 October 2005

Abstract To investigate the mechano-transduction system of cells, we identified genes responsive to a cyclic mechanical stimulus. MC3T3.E1 cells were cultured on a computer-controlled vacuum-pump-operated device designed to provide a cyclic mechanical stimulus. A maximum elongation of 15% of membrane at 10 cycles/min (3 s extension followed by 3 s relax per cycle) was repeated for 48 h. By means of a differential display, the gene expression pattern of cells exposed to the stimulus was compared with that of unexposed cells. As a result, a gene fragment that was exclusively expressed in mechanically stressed cells was identified. By using expressed sequence tag walking together with the oligo-capping method, this gene was identified as phosphatidylinositol 4-phosphate 5-kinase type II β (initially known as *Pip5k2β* but now reclassified as *Pip4k2β*). The specific up-regulation of *Pip4k2β* upon mechanical stimulus was also confirmed by using another apparatus, viz. a computer-controlled linearized-stepping motor system. To examine the involvement of the cyclic mechanical stimulus in the regulation of *Pip4k2β* expression in musculoskeletal tissue, we created an Achilles tendon transection model in rabbits. The temporal expression of *Pip4k2β* was assessed by means of a quantitative reverse-transcribed polymerase chain reaction. In the gastrocnemius muscle, expression of *Pip4k2β* rapidly decreased 1 week after transection but was restored to normal levels at 4 weeks. In the Achilles tendon, however, expression remained decreased until 4 weeks after transection. We suggest that the expression of *Pip4k2β* can be used as a marker for cells receiving a suitable mechanical stimulus.

Keywords Cyclic mechanical stimulus · Differential display · *Pip4k2β* · Mechanical stimulus-responsive genes · Musculoskeletal tissue healing · Rabbit (NZW)

This study was supported by a Grant-in-Aid for Scientific Research from the Ministry of Education, Science, Sports and Culture of Japan.

S. Sano · A. Okawa · A. Nakajima · M. Tahara · K. Fujita · Y. Wada · M. Yamazaki · H. Moriya · T. Sasho (✉)
Department of Orthopaedic Surgery,
Graduate School of Medicine,
Chiba University, 1-8-1 Inohana,
Chuo-ku, Chiba, 260-8677, Japan
e-mail: sasho@faculty.chiba-u.jp
Tel.: +81-43-226-2117
Fax: +81-43-226-2116

Introduction

Cells and tissues are constantly exposed to mechanical stimuli in many parts of the body. A number of attempts have recently been made to understand the biological and physiological roles that mechanical stimuli might play in many aspects of cellular functions (Benjamin and Hillen 2003; Daffara et al. 2004; Martinac 2004).

Investigators have reported the importance of mechanical stimuli not only during development (Elder et al. 2000; Robling et al. 2001; Wang and Mao 2002) and in the overall maintenance of physiological homeostasis (Rubin et al. 2001, 2002), but also in disease development (Park et al. 1998). Examination of the mechanisms by which the induction of gene expression is regulated by mechanical stimuli allows us to determine the way that cells respond to mechanical stimuli and the manner in which these stimuli are converted into intra-cellular signals. Moreover, accumulation of specific knowledge regarding the transcriptional regulation of MSR (mechanical stimulus-responsive) genes might improve our understanding of their roles in numerous cell regulatory contexts.

MSR genes are well known to play important roles in the signal transduction of endothelial cells, osteoblasts, fibroblasts, smooth muscle cells and cardiac muscle cells (Birukov et al. 1995; Danciu et al. 2003; Naruse et al. 1998; Sai et al. 1999); however, a number of known and/or unknown genes might not yet have been characterized as MSR genes. Furthermore, few reports have assessed the roles of MSR genes in vivo.

In musculoskeletal tissue healing, the tendon and muscle regeneration process begins immediately after their injury.

Once they are healed and gain continuity, they can transmit the physiological force to cells of the tendon and the muscle, thereby enabling them to receive mechanical stimuli once again. Based on this, we have hypothesized that the expression of MSR genes would be robust in intact tendon and muscle, attenuated when the tendon or muscle is transected and then increased as they heal. This could be clinically relevant to future treatments for musculoskeletal injury, because the expression levels of MSR genes would allow us to know to what extent injured tendon and muscle have healed and recovered their function.

With this goal in mind, we initially identified an MSR gene responsive to a cyclic mechanical stimulus by means of a differential display and then determined the full length cDNA sequence of the gene. Its responsiveness to a cyclic mechanical stimulus was tested by using two different in vitro systems and an in vivo model.

Materials and methods

Cells and cell culture

Five osteoblastic cell lines were cultured in a computer-controlled vacuum-pump-operated device (Flexercell, Flexcell, McKeesport, Pa.). MC3T3.E1 cells were provided courtesy of Dr. Kodama (Ohu University, Koriyama, Japan). Cells were cultured in RPMI-1640 (Gibco BRL, Gaithersburg, Md.) containing 10% fetal calf serum and grown under 5% $C0_2$ at 37°C.

Cell culture under a cyclic mechanical stimulus

To culture MC3T3.E1 cells under a cyclic mechanical stimulus, we used a computer-controlled vacuum-pump-operated device equipped with a specially designed microplate (FLEX-I, Flexcell) containing a deformable elastic silicone film lying at the bottom. Rigid-bottomed plates (FLEX-II, Flexcell) were used for control cultures.

Specifically, when the pump draws in air, the bottom of the experimental plate bulges and, when the valve shuts off, it flattens. Cells attached to the [illegible]

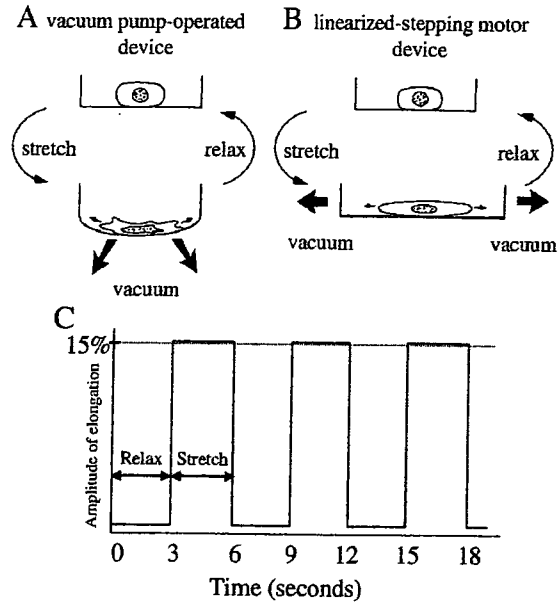

Fig. 1 Mechanical stimulus provided by two different pieces of apparatus. **A** The Flexercell computer-controlled vacuum-pump-operated device allows the cells to stretch and relax cyclically in response to the stimulus. **B** The NS-300 computer-controlled linearized-stepping motor device allows cells to stretch and relax in one direction by the computer-controlled linearized-stepping motor. **C** Mechanical stimulus parameters (*stretch, reflex*). A maximum elongation of 15% at 10 cycles/min (3 s extension followed by 3 s relax per cycle) was repeated over 48 h

relaxes cells cyclically. MC3T3.E1 cells were allowed to attach to deformable rectangular plates designed for this machine and were stretched and relaxed in one direction by a computer-controlled linearized-stepping motor system (Fig. 1b). Both ends of the chamber were firmly attached to a movable frame, which was connected to a motor-driven shaft. The amplitude and frequency of stretch was controlled by a programmable microcomputer. The silicon membrane was uniformly stretched over the whole membrane area and lateral thinning did not exceed 1% at 15% stretch. The stimulus parameters and other conditions used for this machine were the same as those used for the vacuum-pump-operated system. Following [illegible]

manufacturer's instructions and blotted onto a nylon membrane (HybondTM-N+, Amersham Pharmacia Biotech., Piscataway, N.J.). The expression levels of the candidate gene fragments were then compared.

Analysis of gene expression for *Pip4k2β* in an in vivo model

NZW rabbits (9–10 weeks old) were used to create an Achilles tendon transection model. In short, a 1.5-cm longitudinal skin incision was made on the distal end of the right hind limb of rabbits and the Achilles tendon was cut transversely at the calcaneus attachment portion. In this model, the tendon healed and started to become functional 4 weeks after transection (S. Sano et al., unpublished). Fifteen rabbits were used; five rabbits were sacrificed at 1 and 4 weeks and five rabbits were sham-operated and used as controls. When harvesting the Achilles tendon, special care was taken to dissect only the tendinous portion far from the newly formed granular tissue at the injured site. The gastrocnemius muscle sample was also taken from the centre of the muscle belly. These experimental procedures were performed under the approval of the Animal Care and Use Committee of Chiba University.

Total RNA was extracted from the tendon and the gastrocnemius muscle by using Trizol (Gibco BRL). Gene expression of *Pip4k2β* was examined by quantitative RT-PCR with primers (C)/(E) (see Fig. 3). Following standard Southern blotting, the radioactivity of hybridized bands was quantified by utilizing a bio-image analyzer (Image Gauge, Fujifilm, Tokyo, Japan) and the relative expression levels of *Pip4k2β* to β-actin were calculated. Statistical analysis was performed with Fisher's protected least significant differences at a level of significance of $P<0.05$.

Results

Mechanical stimulus responsiveness of cell line

MC3T3.E1 cells responded to cyclic stretching and relaxation with a morphological change. Specifically, after the stimulus, cells grew in concentric circles. We used MC3T3.E1 cells for further experiments.

Cloning of a gene fragment responsive to the cyclic mechanical stimulus and Northern blot analysis

More than 1000 bands were identified on a differential display gel. Among them, relative to control cells, five bands were expressed more highly in cells exposed to the mechanical stimulus. Subsequently, we investigated the expression of each fragment by Northern blot analysis. One of them showed exclusive expression in cells exposed to the stimulus and no expression in unexposed cells. This fragment was tentatively named 103A.2b. However, one fragment, named FG1a, was a false-positive (Fig. 2a).

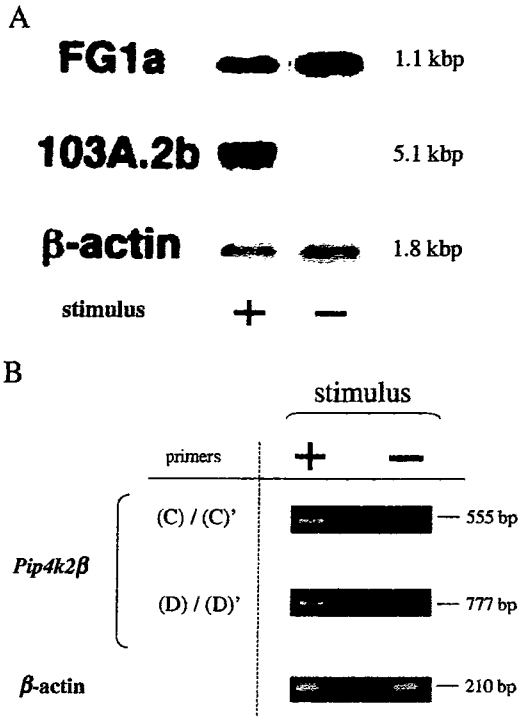

Fig. 2 **A** Exclusive expression of gene fragment 103.A2 in cells exposed to the cyclic mechanical stimulus. Total RNA was extracted from two sources (MC3T3.E1 cells cultured under a cyclic mechanical stimulus and those cultured quiescently) for Northern blot analysis. FG1a and 103A.2b were cloned gene fragments derived from the differential display and were used as probes. 103A.2b was exclusively expressed in cells exposed to a cyclic mechanical stimulus but FG1a was a false positive. Experiments were performed three times and representative data are shown. **B** Reproducibility of the mechanical stimulus responsiveness of *Pip4k2β* by using another type of stimulus. Up-regulation of *Pip4k2β* induced by a cyclic mechanical stimulus was verified by employing a linearized-stepping motor device (NS-300). Two sets of RT-PCR were performed with different primers (C)/(C') and (D)/(D') (Fig. 3). Intensive up-regulation of *Pip4k2β* was detected in cells exposed to the stimulus but not in cells which did not receive the stimulus. Experiments were performed three times and representative data are shown

Determination of the full-length cDNA sequence of the MSR gene

The 103A.2b fragment was 206 bp in length. No sequence similarity was found between 103A.2b and any known genes in the database. Therefore, expressed sequence tag (EST) walking was performed. An EST contig was extended to 3.6 kb until the 5'-end showed sequence similarity with *PIPKIIβ* (*Mus musculus* phosphatidylinositol phosphate kinase type II β, partial cds, Gen-Bank accession no. AB054987; between & and & in Fig. 3). Moreover, we found that the 5'-end of *PIPKIIβ* had sequence similarity with *Pip5k2β* (*Mus musculus* phosphatidylinositol-4-phosphate 5-kinase type II β, partial cds, Gen-Bank accession no. AY050219; between # and # in Fig. 3). The sequence continuity of 103A.2b, the EST contig, *PIPKIIβ* and *Pip5k2β* were confirmed by three sets of RT-PCR with primers (A)/(A'), (B)/(B') and (C)/(C')

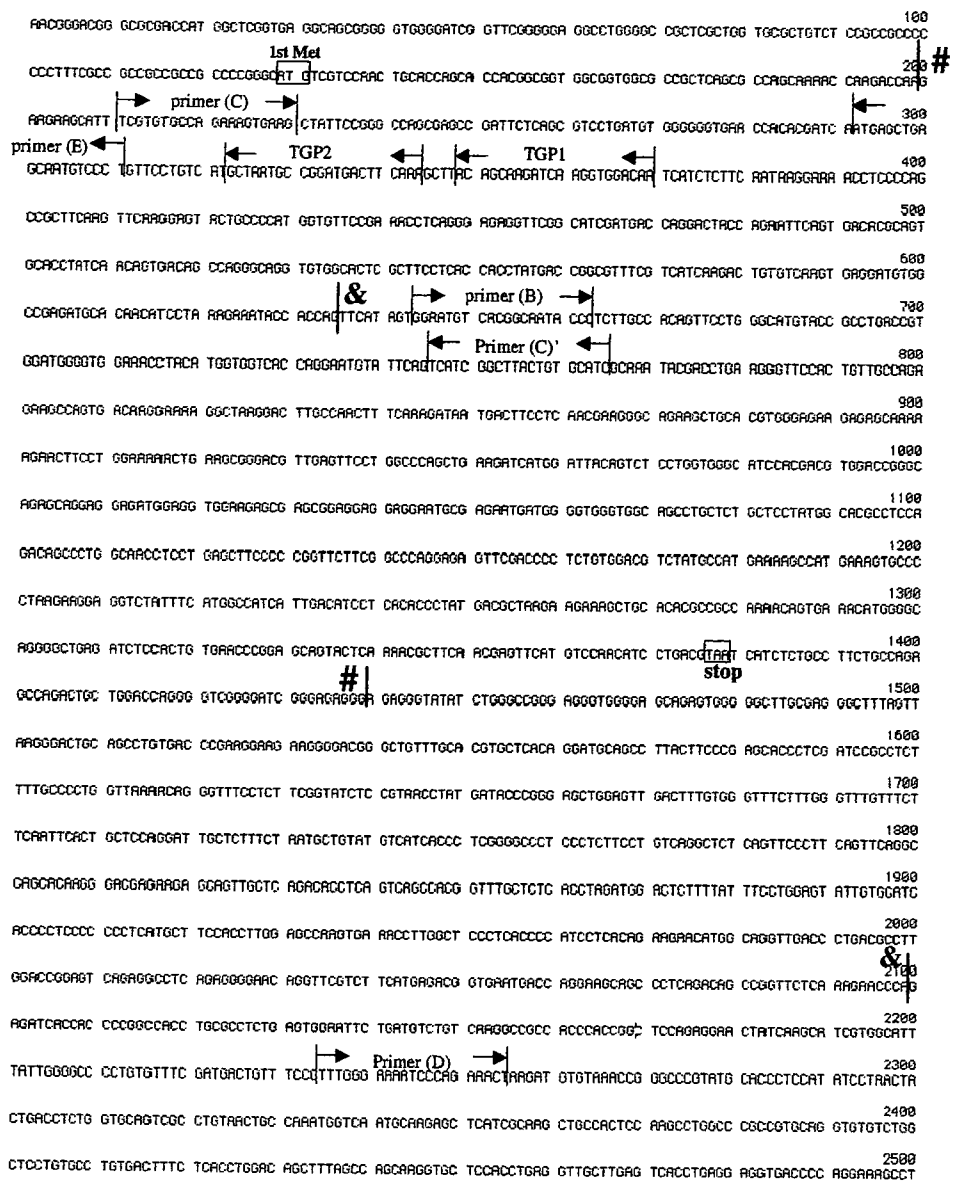

Fig. 3 Full-length 5043-bp cDNA sequence of the *Pip4k2β* gene. The 1st Met and the stop codon are each represented by a *rectangle*. 103A.2b, a 206-bp fragment identified by differential display, is *underlined*. Partial cDNA sequences registered as *PIPKIIβ* and *Pip5k2β* in the Gen-Bank correspond to nucleotide nos. 636-2099 (between & and &) and 200-1439 (between # and #), respectively. The sequences and directions for specific primers used in this study are also shown

(Fig. 3) with the mouse skeletal muscle being used as an RNA source. The transcription initiation site was determined by using the oligo-capping method (Maruyama and Sugano 1994) with Cap Site cDNA Mouse Skeletal Muscle (Nippon Gene, Tokyo, Japan) and the specific primers of TGP-1and-2 (Fig. 3). Thus, we determined that the full-length of the gene was 5043 bp and included a coding region of 1251 bp (nucleotide nos. 129-1379; Fig. 3). Since *Pip5k2β* is now reclassified as *Pip4k2β* (Rameh et al. 1997), we defined this gene as *Pip4k2β*. The strategy by which we determined the full-sequence is summarized in Fig. 4.

Reproducibility of the cyclic mechanical stimulus responsiveness of *Pip4k2β* by using another type of stimulus

Total RNA was extracted from cells cultured under the cyclic mechanical stimulus provided by the linearized-stepping motor device (NS-300) and those cultured quiescently. Two sets of RT-PCR was performed with different primers (C)/(C') and (D)/(D') (Fig. 3). Both of them showed intensive up-regulation of *Pip4k2β* in cells exposed to the stimulus; however, no expression was detected in cells that did not receive the stimulus (Fig. 2b).

Fig. 3 (continued)

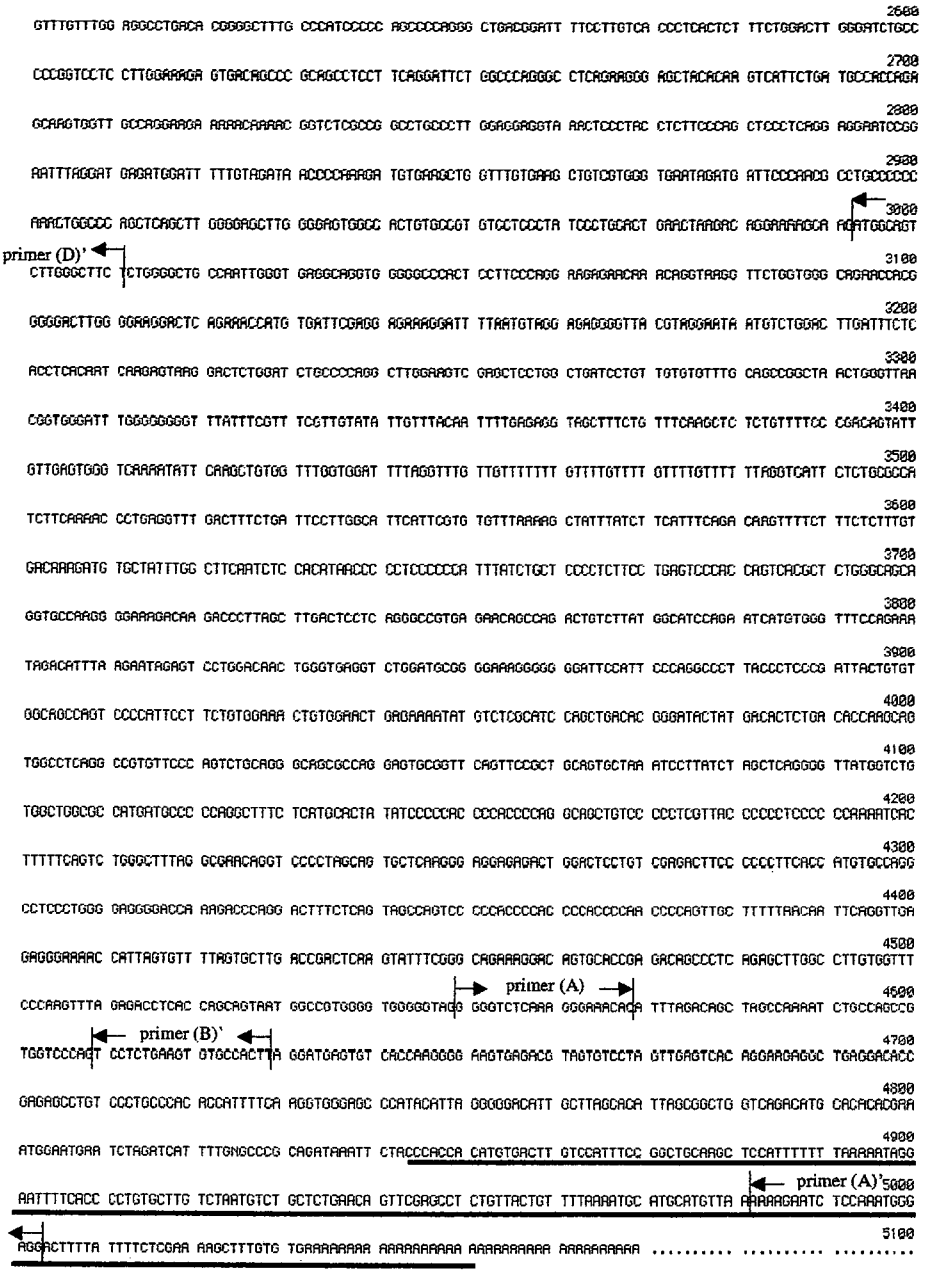

Temporal expression of *Pip4k2β* during Achilles tendon healing

Before transection (i.e. in a control), expression of *Pip4k2β* was clearly detected both in the gastrocnemius muscle and in the Achilles tendon (Fig. 5a,b). After transection, the expression levels of *Pip4k2β* in the gastrocnemius muscle rapidly decreased to 40% of control at 1 week but were restored to normal at 4 weeks (Fig. 5a). Similarly, the expression levels in the Achilles tendon decreased to 25% of control at 1 week; however, it remained decreased until 4 weeks after transection (Fig. 5b).

Discussion

Recently, increasing attention has been paid to the relationship between mechanical stimuli and cellular responses. Previous studies designed to investigate cellular responses to mechanical stimuli in vitro have revealed that cells in a culture dish proliferate and rearrange themselves (Brighton et al. 1991; Buckley et al. 1988). Furthermore, the development of a special device to allow the culture of cells under mechanical stimuli has helped to increase our knowledge of their responses (Neidlinger-Wilke et al. 1994).

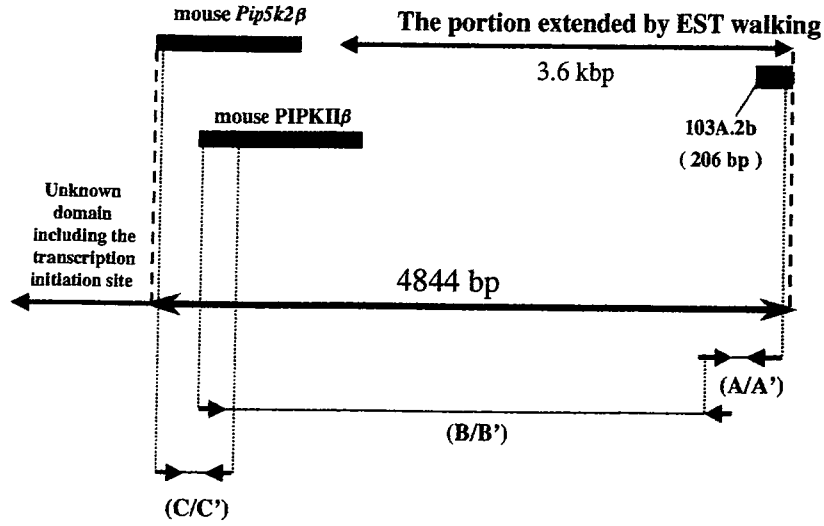

Fig. 4 Strategy for the determination of the full-length cDNA sequence of the *Pip4k2β* gene. Repeated BLAST homology searches of the EST database in an upstream direction was used to extend the 103A.2b fragment to 3.6 kb. The 5'-portion of this fragment was identical to mouse *PIPKIIβ*. Similarly, the 5'-portion of *PIPKIIβ* was identical to mouse *Pip5k2β*. Their sequence continuity was confirmed by three sets of RT-PCR with primers (A)/(A'), (B)/(B') and (C)/(C'). A 200-bp sequence further upstream that included the transcription initiation site was determined by the oligo-capping method

As in previous studies, we used a computer-controlled vacuum-pump-operated device in the first part of our study. However, as has been reported, cells grown on this apparatus do not necessarily receive homogeneous stimuli in terms of direction and magnitude (Gilbert et al. 1994; Waters et al. 2001). Therefore, from our first experiment alone, we could not determine the magnitude of stretch that induced *Pip4k2β*. In addition, we could not refute the possibility of false-positives, even after having confirmed exclusive expression by Northern blot analysis. Thus, we further cultured cells on a different device in which they received a more homogeneous stimulus. This clearly verified that *Pip4k2β* was specifically induced in the presence of a cyclic mechanical stimulus.

Previous reports have shown that a transcription factor, nuclear factor kappa B (NFkB), is an important mediator for the induction of MSR genes (Chaqour et al. 1999; Inoh et al. 2002). Therefore, we examined whether NFkB-binding sites were present in the putative promoter region of the *Pip4k2β* gene. Indeed, we identified a candidate NFkB-binding site, a GGGGAGGCCT sequence in the putative promoter region (nucleotide nos. 56-65; Fig. 3), suggesting NFkB-mediated up-regulation of *Pip4k2β*. However, promoter analysis, such as the luciferase assay, is required to elucidate the involvement of NFkB in the regulation of *Pip4k2β* expression. *Pip4k2β* encodes type II phosphatidylinositol phosphate (PIP) kinase, which in turn produces phosphatidylinositol 4,5 bisphosphate (PI4,5P_2),

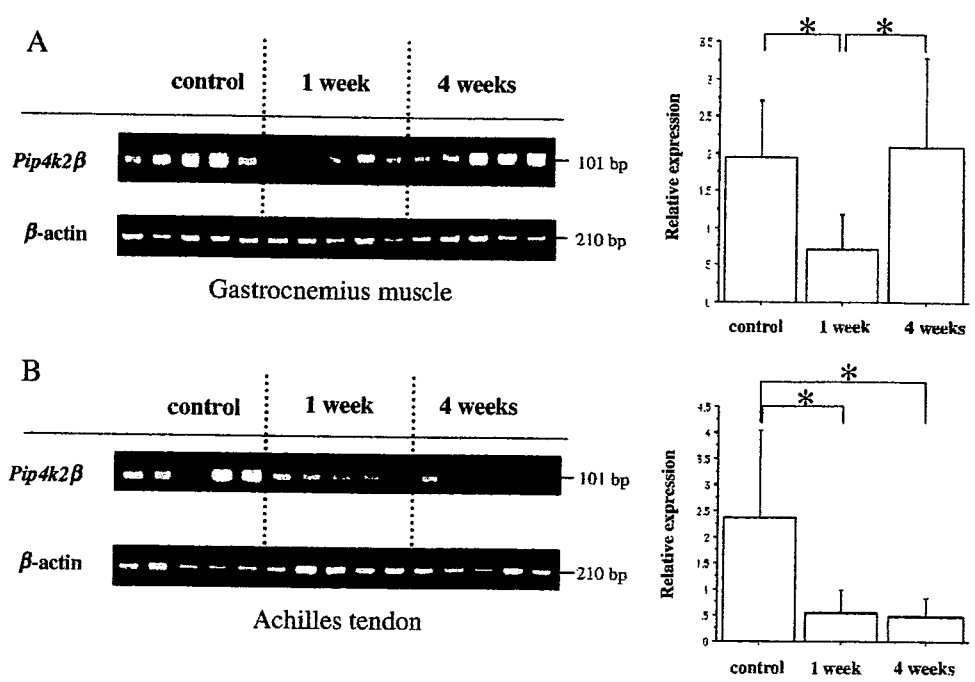

Fig. 5 Temporal expression of *Pip4k2β* during Achilles tendon healing. Expression of *Pip4k2β* in the gastrocnemius muscle (**a**) and Achilles tendon (**b**) was monitored by RT-PCR after transection. Five rabbits were sacrificed at different time-points. Relative expression levels of *Pip4k2β* to β-actin are also shown. **a** Expression of *Pip4k2β* in the gastrocnemius muscle rapidly decreased 1 week after transection and was restored to normal at 4 weeks. **b** In the Achilles tendon, expression also decreased at 1 week but it remained decreased until 4 weeks. Experiments were performed three times and representative data are shown. Values are expressed as a mean±SD. *Significantly different from control, $P<0.05$

which utilizes PI5P as a substrate. $PI4,5P_2$ is a crucial second messenger that regulates a myriad of cellular activities, including modulation of the actin cytoskeleton, vesicle trafficking, focal adhesion formation and nuclear events (Doughman et al. 2003). Although the functional role of Pip4k2β under physiological conditions has not been fully elucidated, Luoh et al. (2004) have demonstrated that overexpression of *Pip4k2β* in breast cancer cell lines confers proliferation advantage and promotes anchorage-independent growth and they imply that *Pip4k2β* plays important roles in the development and/or progression of breast cancer. In the present study, we have used MC3T3. E1 cells but the cells exposed to the cyclic mechanical stimulus show increased proliferation activity compared with those not exposed (data not shown). We therefore speculate that the specific up-regulation of *Pip4k2β* observed in the cells exposed to the cyclic mechanical stimulus might contribute to their proliferation.

To assess the involvement of the cyclic mechanical stimulus in the regulation of *Pip4k2β* in vivo, we first examined the tissue distribution of its expression under physiological normal conditions by Northern blot analysis. Expression was observed in the heart, brain, lung, liver, kidney and skeletal muscle but not in spleen and testis (data not shown). We speculate that, in brain, liver and kidney, which are abundantly vascular, the cyclic changes in blood pressure exerted on the endothelial cells induces the expression of *Pip4k2β*, although factors other than cyclic mechanical stimulus might also be involved in controlling the expression levels of this gene.

Next, we investigated whether the loss of mechanical stimulus could attenuate the expression of *Pip4k2β* by using the Achilles tendon transaction model. Loss of the mechanical stimulus indeed induced a rapid reduction of *Pip4k2β* expression both in the tendon and the muscle. Moreover, expression of *Pip4k2β* in the muscle was restored to normal 4 weeks after transection and appeared to be healed as evidenced by the functioning of the animals. These observations support the idea that *Pip4k2β* is synthesized under mechanically normal physiological conditions and that its production decreases concomitantly with the loss of a suitable mechanical stimulus. Although the expression of *Pip4k2β* might have reflected other factors than the mechanical stimulus, taken together with our in vitro results that *Pip4k2β* is intensely expressed in cells exposed to the cyclic mechanical stimulus, *Pip4k2β* seems to be, in part, involved in the recovery of mechanical stimulus responsiveness during Achilles tendon healing. Contrary to our expectations, expression in the tendon was not restored to normal at 4 weeks after transection. We speculate that an adhesive change, which occurred around the transected tendon, could have disturbed the transmission of the physiological force to the tendon cells. Another possibility is that a time-point of 4 weeks is too early for tendon cells to re-express the normal levels of *Pip4k2β*. Further evaluations of the expression levels of *Pip4k2β* at later stages of healing will therefore be needed.

In this study, we have reported, for the first time, that *Pip4k2β* is one of the MSR genes. Its specific up-regulation upon mechanical stimulus has been verified by using two different in vitro systems and an in vivo model. Further studies are required to elucidate the molecular mechanism by which a cyclic mechanical stimulus induces the expression of *Pip4k2β* and to establish its role under physiological conditions. Our results also indicate the possible usefulness of the *Pip4k2β* gene as a marker for monitoring functional musculoskeletal tissue healing.

Acknowledgements We express our sincere gratitude to Dr. R. L. Sah for helpful discussions and Dr. H. Sakai for assistance with the cell cultures. We also thank A. P. Lestick and B. Baehr for editorial assistance.

References

Benjamin M, Hillen B (2003) Mechanical influences on cells, tissues and organs–"mechanical morphogenesis". Eur J Morphol 41: 3–7

Birukov KG, Shirinsky VP, Stepanova OV, Tkachuk VA, Hahn AW, Resink TJ, Smirnov VN (1995) Stretch affects phenotype and proliferation of vascular smooth muscle cells. Mol Cell Biochem 23:131–139

Brighton CT, Strafford B, Gross SB, Leatherwood DF, Williams JL, Pollack SR (1991) The proliferative and synthetic response of isolated calvarial bone cells of rats to cyclic biaxial mechanical strain. J Bone Joint Surg [Am] 73:320–331

Buckley MJ, Banes AJ, Levin LG, Sumpio BE (1988) Osteoblasts increase their rate of division and align in response to cyclic, mechanical tension in vitro. Bone Miner 4:225–236

Chaqour B, Howard PS, Richard CF, Macarak EJ (1999) Mechanical stretch induces platelet activating factor receptor gene expression through the NF-kB transcription factor. J Mol Cell Cardiol 31:1345–1355

Daffara R, Botto L, Beretta E, Conforti E, Faini A, Palestini P, Miserocchi G (2004) Endothelial cells as early sensors of pulmonary interstitial edema. J Appl Physiol 97:1573–1583

Danciu TE, Adam RM, Naruse K, Freeman MR, Hauschka PV (2003) Calcium regulates the PI3K-Akt pathway in stretched osteoblasts. FEBS Lett 11:193–197

Doughman RL, Firestone AJ, Anderson RA (2003) Phosphatidylinositol phosphate kinases put $PI4,5P_2$ in its place. J Membr Biol 194:77–89

Elder SH, Kimura JH, Soslowsky LJ, Lavagnion M, Goldstein SA (2000) Effect of compressive loading on chondrocyte differentiation in agarose cultures of chick limb-bud cells. J Orthop Res 18:78–86

Gilbert JA, Weinhold PS, Banes AJ, Link GW, Jones GL (1994) Strain profiles for circular plates containing flexible surfaces employed to mechanically deform cells in vitro. J Biomech 27:1169–1177

Inoh H, Ishiguro N, Sawazaki S, Amma H, Miyazu M, Iwata H, Sokabe M, Naruse K (2002) Uni-axial cyclic stretch induces the activation of transcription factor nuclear factor kappaB in human fibroblast cells. FASEB J 16:405–407

Liang P, Pardee A (1992) Differential display of eukaryotic messenger RNA by means of the polymerase chain reaction. Science 257:967–971

Luoh SW, Venkatesan N, Tripathi R (2004) Overexpression of the amplified Pip4k2β gene from 17q11-12 in breast cancer cells confers proliferation advantage. Oncogene 23:1354–1363

Martinac B (2004) Mechanosensitive ion channels: molecules of mechanotransduction. J Cell Sci 117:2449–2460

Maruyama K, Sugano S (1994) Oligo-capping. A simple method to replace the cap structure of eukaryotic mRNAs with oligoribonucleotides. Gene 138:171–174

Naruse K, Yamada T, Sai XR, Hamaguchi M, Sokabe M (1998) Pp125FAK is required for stretch dependent morphological response of endothelial cells. Oncogene 30:455–463

Neidlinger-Wilke C, Wilke HJ, Class L (1994) Cyclic stretching of human osteoblasts affects proliferation and metabolism: a new experimental method and its application. J Orthop Res 12: 70–78

Park JM, Borer JG, Freeman MR, Peters CA (1998) Stretch activates heparin-binding EGFlike growth factor expression in bladder smooth muscle cells. Am J Physiol 275:C1247–1254

Rameh LE, Tolias KF, Duckworth BC, Cantley LC (1997) A new pathway for synthesis of phosphatidylinositol-4, 5-bisphosphate. Nature 390:192–196

Robling AG, Duijvelaar KM, Geevers JV, Ohashi N, Turner CH (2001) Modulation of appositional bone growth in the rat ulna by applied static and dynamic force. Bone 29:105–113

Rubin C, Turner AS, Basin S, Mallinckrodt C, McLead K (2001) Anabolism. Low mechanical signals strengthen long bones. Nature 412:603–604

Rubin C, Turner AS, Muller R, Mittra E, McLeod K, Lin W, Qin YX (2002) Quantity and quality of trabecular bone in the femur are enhanced by a strongly anabolic, noninvasive mechanical intervention. J Bone Miner Res 17:349–357

Sai X, Naruse K, Sokabe M (1999) Activation of pp60 (src) is critical for stretch-induced orienting response in fibroblasts. J Cell Sci 112: 1365–1373

Wang X, Mao JJ (2002) Accelerated chondrogenesis of the rabbit cranial base growth plate by oscillatory mechanical stimuli. J Bone Miner Res 17:1843–1850

Waters CM, Glucksberg MR, Lautenschlager EP, Lee CW, Van Marte RM, Warp RJ, Savla U, Healy KE, Moran B, Castner DG, Bearinger JP (2001) A system to impose prescribed homogenous strains on cultured cells. J Appl Physiol 91: 1600–1610